Research Article

Computer-Aided Design and Biological Evaluation of Diazaspirocyclic D$_4$R Antagonists

Caleb A. H. Jones,*,¶ Benjamin P. Brown,¶ Daniel C. Schultz,¶ Julie Engers, Valerie M. Kramlinger, Jens Meiler,* and Craig W. Lindsley*

Cite This: ACS Chem. Neurosci. 2024, 15, 2396−2407
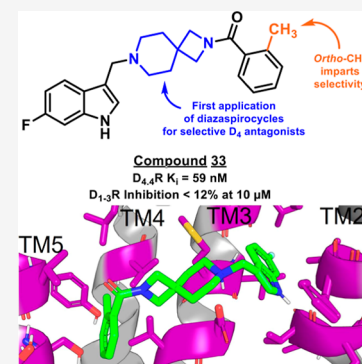
Read Online

ACCESS | Metrics & More | Article Recommendations | Supporting Information

ABSTRACT: Parkinson's disease (PD) is a neurodegenerative disorder characterized by the progressive loss of dopaminergic neurons in the substantia nigra, resulting in motor dysfunction. Current treatments are primarily centered around enhancing dopamine signaling or providing dopamine replacement therapy and face limitations such as reduced efficacy over time and adverse side effects. To address these challenges, we identified selective dopamine receptor subtype 4 (D$_4$R) antagonists not previously reported as potential adjuvants for PD management. In this study, a library screening and artificial neural network quantitative structure−activity relationship (QSAR) modeling with experimentally driven library design resulted in a class of spirocyclic compounds to identify candidate D$_4$R antagonists. However, developing selective D$_4$R antagonists suitable for clinical translation remains a challenge.

First application of diazaspirocycles for selective D$_4$ antagonists

Ortho-CH$_3$ imparts selectivity

Compound 33
D$_{4.4}$R K$_i$ = 59 nM
D$_{1-3}$R Inhibition < 12% at 10 μM

KEYWORDS: dopamine receptors, D$_4$R antagonism, Parkinson's disease

INTRODUCTION

Parkinson's disease (PD) is a debilitating neurodegenerative disorder characterized by progressive motor dysfunction resulting from the degeneration of dopaminergic neurons in the substantia nigra.[1,2] The resulting dopamine deficiency leads to the classic motor symptoms of PD, including bradykinesia, resting tremors, and rigidity.[1] While current treatments, such as enhancing dopamine signaling and providing dopamine replacement therapy, have been effective in alleviating motor symptoms in the early stages of PD, the need for innovative therapeutic approaches is underscored by the challenges of maintaining their long-term efficacy and minimizing the risk of side effects, including medication-induced dyskinesias.[2,3] One promising avenue of exploration lies in the design and development of selective dopamine receptor subtype 4 (D$_4$R) antagonists as potential adjuvants for PD management.[4−6]

Dopamine receptors are divided into two families based on structural similarities, function, and pharmacological properties: the D$_1$-like receptor family, which includes primarily the D$_1$R and D$_5$R subtypes, and the D$_2$-like receptor family, which includes D$_2$R, D$_3$R, and D$_4$R.[7−9] Functionally, these two families have opposing mechanisms, with D$_1$-like receptors stimulating adenyl cyclase through G$_{\alpha s}$ signaling and D$_2$-like receptors inhibiting adenyl cyclase through G$_{\alpha i/o}$ signaling.[7] Further receptor subtype heterogeneity can be found at the level of genetic polymorphisms. D$_4$R itself comprises 10 different genotypes, with D$_{4.2}$, D$_{4.4}$, and D$_{4.7}$ being the most

prevalent of these.[10−12] The pharmacological management of PD currently focuses primarily on enhancing dopamine signaling through D$_2$R, such as by providing dopamine precursor therapy with levodopa or through direct agonism with pramipexole or ropinirole.[13−25]
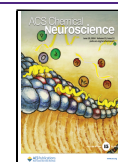
D$_4$R has garnered increasing attention in recent years due to its distinctive expression pattern within the central nervous system and its potential role in modulating dopamine signaling.[5,6,26] Unlike other dopamine receptor subtypes, D$_4$R is primarily located in the frontal cortex and limbic system, areas that are associated with cognitive and emotional processes, and consequently has been implicated largely in neuropsychiatric conditions (though D$_4$R is also expressed in the periphery).[27−40] Early D$_4$R antagonists were considered as potential therapeutic avenues for diseases such as addiction and attention-deficit/hyperactivity disorder (ADHD).[41−44] Additionally, due to the expression of D$_4$R within the basal ganglia, which is associated with the development of dyskinesias in PD patients, research has also unveiled the involvement of D$_4$R in motor control, making it a compelling target in the context of PD for the treatment of levodopa-
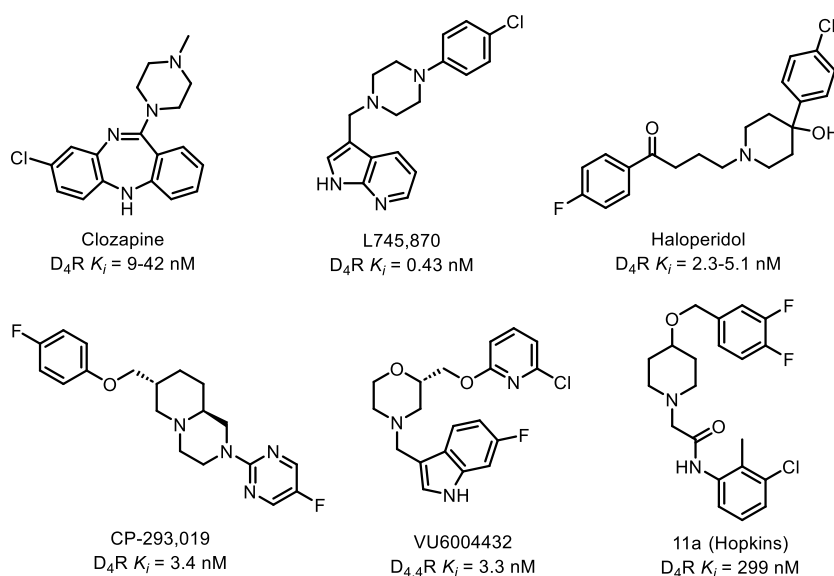
Clozapine
D_4R K_i = 9-42 nM

L745,870
D_4R K_i = 0.43 nM

Haloperidol
D_4R K_i = 2.3-5.1 nM

CP-293,019
D_4R K_i = 3.4 nM

VU6004432
$D_{4.4}R$ K_i = 3.3 nM

11a (Hopkins)
D_4R K_i = 299 nM

Figure 1. Selected historical compounds demonstrating antagonism at D_4R.[9,30,49−59]
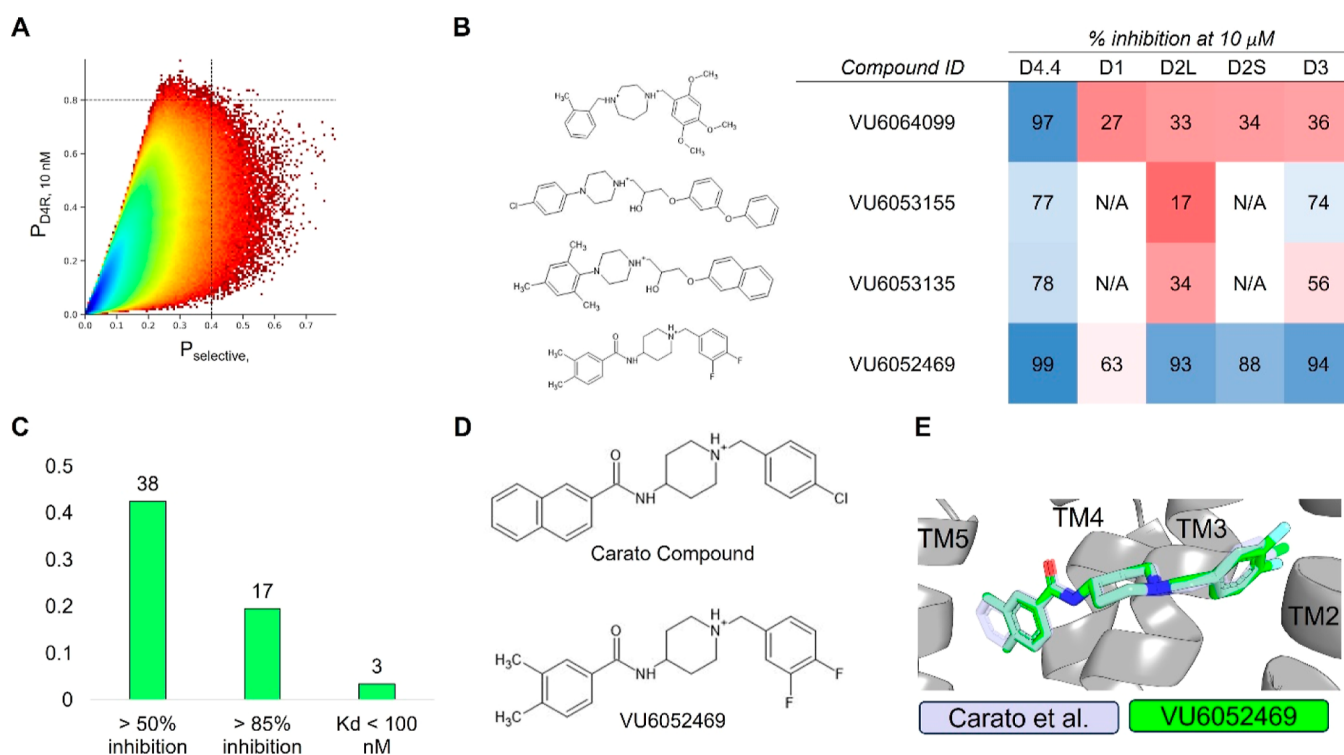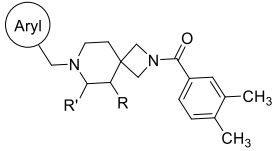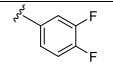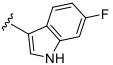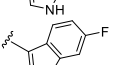
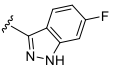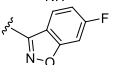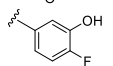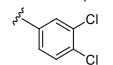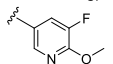Figure 2. Virtual high-throughput screening for D_4R antagonists. (A) Predicted D_4R activity vs selectivity from the ligand-based multitask ANN QSAR model ultralarge library virtual high-throughput screening. Dashed lines indicate QSAR-predicted active classification probabilities at or greater than 80% (horizontal) and 40% (vertical) for D_4R 10 nM activity and overall selectivity, respectively. Plot color is contoured by the density of molecules, with higher-density regions appearing blue and lower-density regions appearing red. (B) Sample molecules identified during the virtual high-throughput screening. (C) D_4R hit-rate for experimentally validated molecules. (D) 2D structures of Carato et al.: compound 22[71] and VU6052469. (E) Overlay of docked poses of Carato et al.: compound 22[71] and VU6052469 within D_4R.

induced dyskinesia (LID).[3,4,33,45−48] Consequentially, interest in the development of selective D_4R antagonists has increased in recent decades, selected examples of which can be seen in Figure 1. The approved antipsychotics clozapine and haloperidol have also been included for reference due to their historical significance, though these are not selective for D_4R.[9,30,49−59]
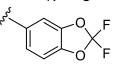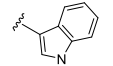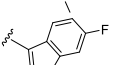
The central challenge in designing D_4R antagonists as an adjuvant therapy for PD lies in obtaining selectivity for D_4R over the other dopamine receptor subtypes, action at which could produce undesired side effects. For instance, antagonism or partial agonism of D_2R has been demonstrated to worsen Parkinsonism, while action at D_1R in conjunction with levodopa administration is associated with increased LID severity.[60−64] Therefore, the pursuit of D_4R antagonists for PD

Table 1. Southern Region SAR

Cmpd No.	Aryl	R	R′	% Inhibition at 10 μM[a]					D4.4 IC$_{50}$ (nM)[a]	D4.4 K$_i$ (nM)[a]
				D4.4	D2S	D2L	D3	D1		
4	(3,4-difluorophenyl)	H	H	88%	8%	9%	9%	21%	2790	250
5	(fluoroindole)	H	H	94%	25%	24%	27%	35%	200	56
6	(fluoroindazole)	H	H	90%	15%	3%	25%	-4%	150	43
7	(fluorobenzisoxazole)	H	H	20%	-	-	-	-	-	-
8	(hydroxy fluorophenyl)	H	H	62%	-	-	-	-	-	-
9	(dichlorophenyl)	H	H	91%	25%	24%	62%	24%	81	22
10	(fluoro methoxy pyridine)	H	H	66%	-	-	-	-	-	-
11	(difluoro benzodioxole)	H	H	66%	-	-	-	-	-	-
12	(indole N-fluorophenyl)	H	H	92%	24%	16%	19%	27%	280	76
13	(fluoroindole)	CH₃	H	85%	-	-	-	-	990	270
14	(fluoroindole)	H	CH₃	89%	-	-	-	-	1920	530

[a]Values were obtained from Eurofins Discovery. See Supporting Information for more details.

therapy demands meticulous attention to the selectivity and efficacy of the designed compounds. Recent advances in synthetic chemistry, structural biology, and pharmacology have enabled the design and characterization of diverse selective D$_4$R antagonists, as exemplified in several key studies.[59,65−69] Building off of these rich structure−activity relationship data, we disclose herein the development of a novel class of potent, selective D$_4$R antagonists suitable for further preclinical optimization.

RESULTS

Ligand-Based Ultralarge Library Screening to Identify Candidate D$_4$R Antagonists. To identify new D$_4$R antagonists, we first performed ligand-based ultralarge library screening using multitask classification artificial neural network (ANN) quantitative structure−activity relationship (QSAR) models (see Computational Methods and Materials in the Supporting Information). We trained four unique QSAR models on publicly available confirmatory screening data (molecules had reported IC$_{50}$ and/or K$_i$/K$_d$ values) from PubChem, one each for D$_2$R, D$_3$R, D$_4$R, and D$_5$R. Each model was trained to predict the likelihood that a molecule is active at or below the following thresholds: 1, 10, 100, 1000, and 10,000 nM. Two primary metrics guided our analysis: (1) the probability that a molecule is active against D$_4$R at or below

10 nM and (2) the predicted selectivity for D$_4$R, where selectivity is given by the equation below.

$$Selectivity = \frac{P_{D_4R,10nM}}{P_{D_4R,10nM} + P_{D_2R,1000nM} + P_{D_3R,1000nM} + P_{D_5R,1000nM}}$$

where $P_{D_4R,10nM}$ is the QSAR-predicted probability of a molecule to be active at or below 10 nM, $P_{D_4R,1000nM}$ is the same metric for D$_2$R at or below 1000 nM, etc. Our formulation of selectivity specifically evaluates the likelihood of a molecule being selective for D$_4$R at 2 orders of magnitude (active at 10 nM D$_4$R vs 1000 nM D$_2$, D$_3$, and D$_5$).

We applied our QSAR models to screen over 1 billion molecules sourced from LifeChemicals and the Enamine REAL database (Figure 2A). Compounds with 10 nM D$_4$R activity prediction scores at or above 0.8 were moved forward for further analysis. Preference was given to compounds also exhibiting a selectivity score exceeding 0.4. We performed property-based flexible alignment[70] of a subset of 500 molecules to the crystallographically bound pose of the D$_4$R-selective antagonist L-745,870,[68] followed by visual inspection. Ultimately, we chose 89 molecules to acquire from Enamine and LifeChemicals for experimental screening at Eurofins Discovery.
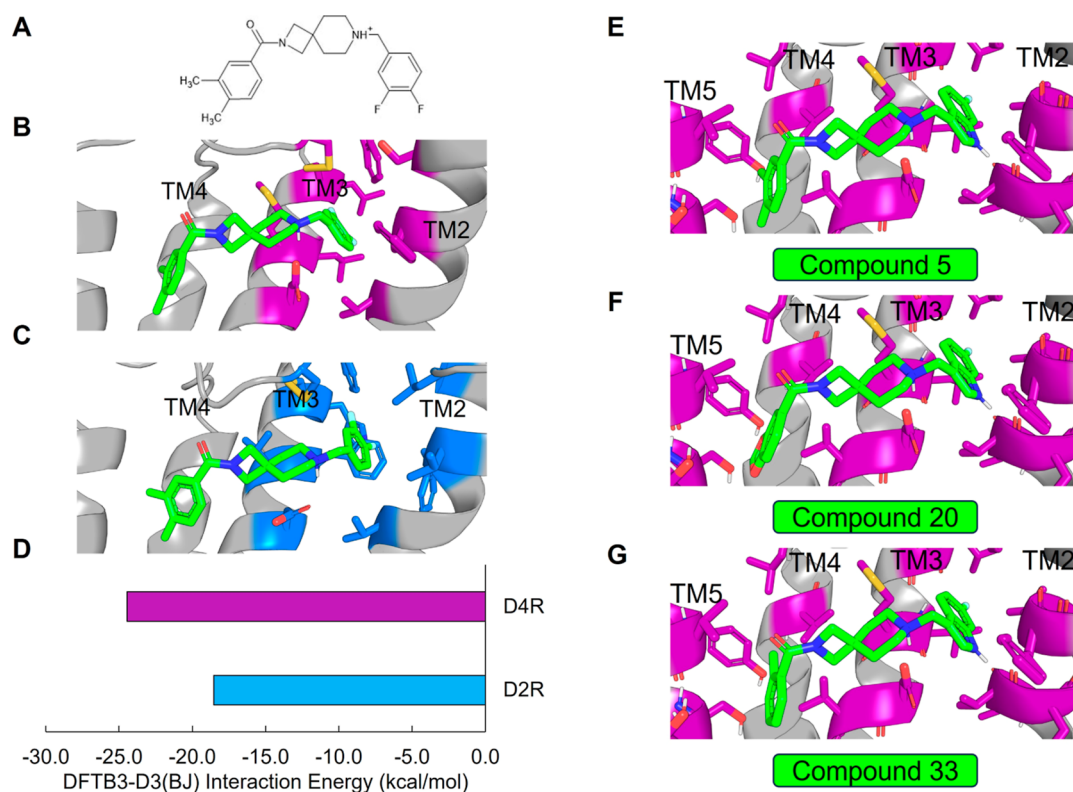
Figure 3. SAR analysis of D_4R selective antagonists. (A) Chemical structure of the spirocyclic compound **4**. (B) Docked pose of compound **4** (green) in D_4R. (C) Docked pose of compound **4** (green) in D_2R. (D) DFTB3-D3(BJ) interaction energy (kcal/mol) between compound **4** and the central aspartate and TM2/TM3 hydrophobic pocket of D_4R (purple) and D_2R (blue). Docked poses of compounds (E) **5**, (F) **20**, and (G) **33**.

Our screening efforts yielded notable outcomes, with 38 of the selected molecules displaying inhibitory activity exceeding 50% at 10 μM and 17 (see Supporting Information for structures) showing greater than 85% inhibition at 10 μM for D_4R (Figure 2B,C). Our success for identifying selective molecules was much lower. This is not unexpected as the selectivity metric is built from multiple independent predictions (eq S1), and thus, error from each prediction accumulates in the final score. Frequently, molecules predicted to be D_4R selective were only selective against a single off-target subtype. Nonetheless, a subset of D_4R-active compounds exhibited varying degrees of selectivity relative to at least one other dopamine receptor subtype (Figure 2B).
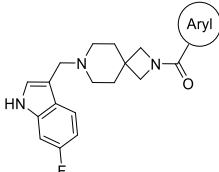
Identification of a Spirocyclic Core for D_4R Antagonists. From our initial screen, we identified compound *VU6052469*, which is structurally similar to a previously published D_4R antagonist by Carato et al. bearing a piperidine core with a naphthamide substituent that exhibits high potency and selectivity for D_4R over D_2R;[71] however, *VU6052469* itself is nonselective (Figure 2B,D). We docked *VU6052469* and the Carato compound into D_4R (PDB ID: 6IQL)[68] to investigate the potential binding mode of our hit (Figure 2E). One challenge with designing D_4R antagonists is the topological pseudosymmetry of D_4R-active compounds, which in the case of *VU6052469* and the Carato compound entails two distal aryl rings linked to a piperidine core (Figure 2D). In principle, this symmetry could enable the molecules to bind such that the halogen-substituted phenyl ring interacts with either transmembrane helices 2 (TM2) and TM3 (Figure S103A) or alternatively with TM4/5/6 (Figure S103B). In either binding pose, for example, *VU6052469* hydrogen bonds with the
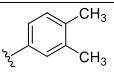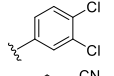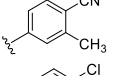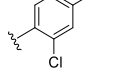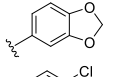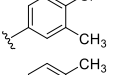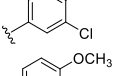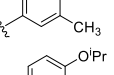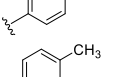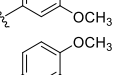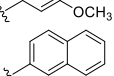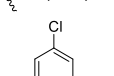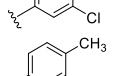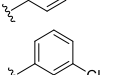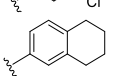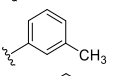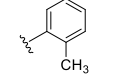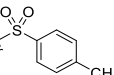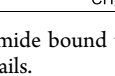
conserved D3.32 side chain, and V3.33 can stack with its aromatic rings (Figure S103). The pocket formed by TM2/3 is hydrophobic and has previously been implicated in ligand selectivity.[68,69] Indeed, the TM2/3 interface differs between D_4R and D_2R in that D_2R contains aromatic ring side chains, while in D_4R, there are aliphatic chains (Figure S104). In contrast, the amino acid composition of TM4/5/6 is a mixture of polar and hydrophobic residues. Notably, a cluster of serine residues engaged in internal backbone hydrogen bonds in TM5/6 renders this portion of the pocket more sterically accessible.

We reasoned that the latter pose is less likely as it induces a greater loss of planarity of the amide linker within the docked pose, which is supported by density functional theory (DFT) conformational stability calculations and molecular orbital analysis performed at the wB97X-D/6-311G(d,p) level of theory[72] (Figure S103C,D). We estimate that the first pose of *VU6052469* (Figure S103A) is 11.3 kcal/mol more energetically favorable, and it follows that the Carato compound adopts a similar binding conformation (Figure 2E). Despite being nonselective, our docked poses suggest that *VU6052469* could readily be made selective through extending the amide bond via a methylene linker and truncating the arene without altering the orientation of the ligand within the binding pocket. To that end, we replaced the secondary amide with an azetidine amide to give a 2,7-diazaspiro[3.5]nonane core, resulting in compound **4**, which displayed selectivity for D_4R with only a partial loss of on-target activity (Table 1).

To better understand the mechanism of selectivity imparted by the spirocyclic core, we docked **4** into D_4R and D_2R (see Supporting Information) (Figure 3A–C). We verified the

Table 2. Northern Ring SAR

Cmpd No.	Aryl	% Inhibition at 10 μM[b]					$D_{4.4}$ IC$_{50}$ (nM)[b]	$D_{4.4}$ K$_i$ (nM)[b]
		$D_{4.4}$	D_{2S}	D_{2L}	D_3	D_1		
5	3,4-dimethylphenyl	94%	25%	24%	27%	35%	200	56
17	3,4-dichlorophenyl	93%	11%	26%	34%	24%	77	21
18	4-cyano-3-methylphenyl	42%	-	-	-	-	-	-
19	2,4-dichlorophenyl	92%	14%	23%	30%	21%	82	23
20	benzodioxole	95%	12%	18%	14%	16%	84	23
21	3-chloro-4-methylphenyl	94%	17%	29%	40%	24%	78	22
22	4-chloro-3-methylphenyl	92%	22%	38%	31%	19%	95	26
23	4-methoxy-3-methylphenyl	78%	-	-	-	-	-	-
24	4-isopropoxyphenyl	63%	-	-	-	-	-	-
25	3-methyl-4-methoxyphenyl	66%	-	-	-	-	-	-
26	3,4-dimethoxyphenyl	14%	-	-	-	-	-	-
27	naphthyl	95%	21%	34%	36%	32%	28	7.6
28	3,5-dichlorophenyl	49%	-	-	-	-	-	-
29	4-methylphenyl	99%	5%	20%	13%	27%	62	17
30	3-chlorophenyl	95%	17%	35%	23%	10%	790	220
31	tetralinyl	93%	22%	26%	35%	21%	260	71
32	3-methylphenyl	92%	18%	18%	12%	10%	490	140
33	2-methylphenyl	93%	0%	-7%	11%	9%	210	59
34[a]	4-methylphenylsulfonyl	94%	17%	50%	49%	47%	120	33

[a]Structure for this compound is a sulfonamide bound to the azetidine nitrogen of the spirocycle. [b]Values were obtained from Eurofins Discovery. See Supporting Information for more details.

binding mode by running molecular dynamics (MD) simulations and analyzing ligand root-mean-square-deviation (rmsd) over time (Figure S105). Our docked poses suggest that the difluorophenyl of **4** differentially engages the TM2/3 hydrophobic pocket in D$_4$R versus D$_2$R. Compared to its complex with D$_4$R, in the D$_2$R complex **4** is shifted deeper into

Scheme 1. Synthesis of Diazaspiro[3.5]nonane D₄R Antagonists
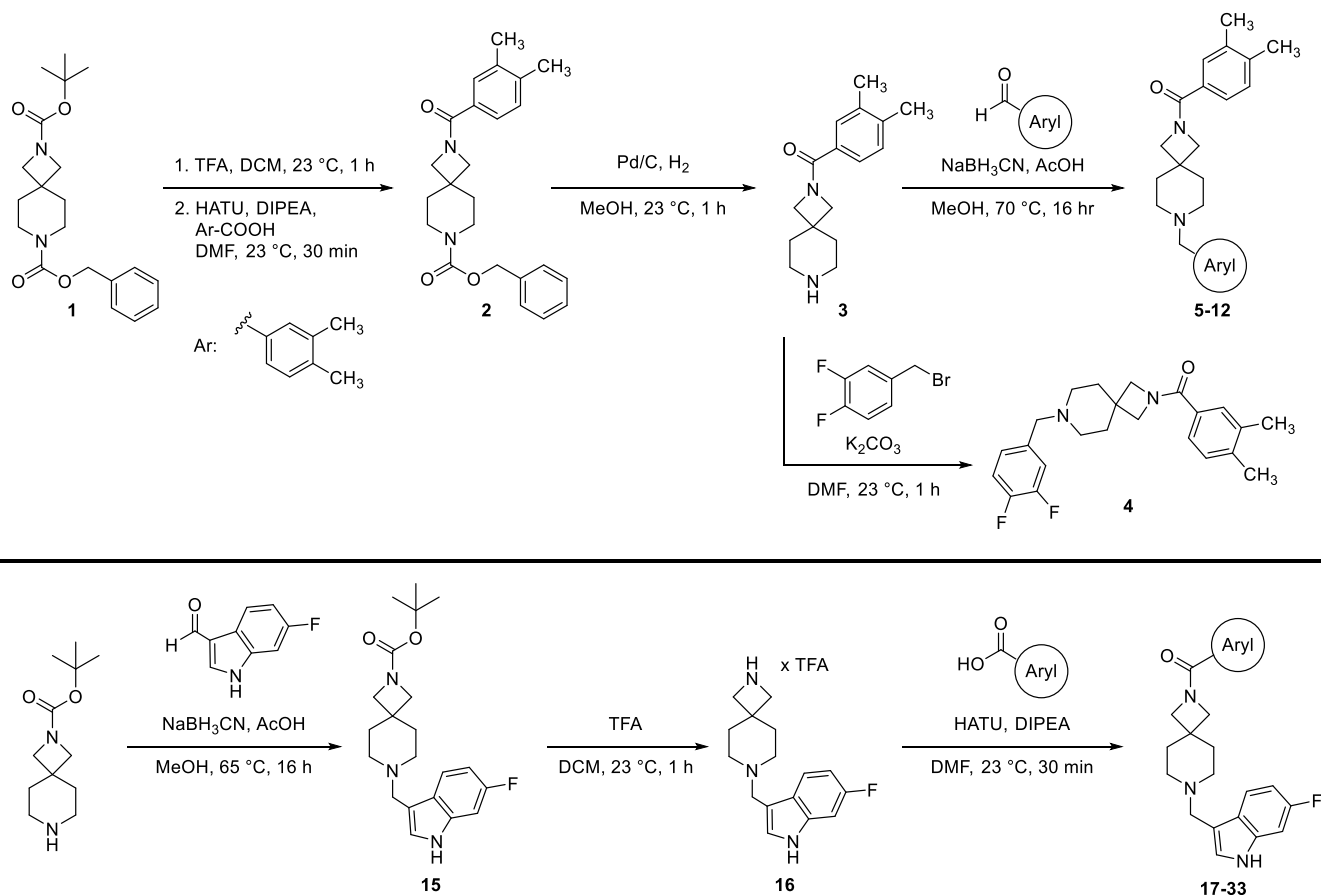
the TM2/3 pocket such that the hydrogen bond geometry between the orthosteric pocket aspartate D3.32 and the protonated piperidine is suboptimal (Figure S106). We confirmed that the D₂R electrostatic interactions are less favorable than D₄R by performing geometry optimization and subsequent interface energy calculations of the complexes using the semiempirical quantum mechanics (QM) tight-binding density functional theory (DFTB) method with dispersion corrections, DFTB3-D3(BJ) (Figure 3D) (see Supporting Information).[73,74] The interaction energies of **4** with respect to the conserved central aspartate D3.32 and TM2/3 hydrophobic pocket in D₄R and D₂R are estimated to be −24.46 and −18.53 kcal/mol, respectively (Figure 3D).

Optimization of Spirocyclic D₄R Antagonist Potency and Selectivity. We sought to improve upon the potency and selectivity of **4** by screening analogues with differing polar aromatic or heteroaromatic groups on the southern end of the compound, installing methyl groups at the 2 or 3 position of the piperidine and probing the effect of the substitution pattern and substituent type on the northern phenyl ring on activity (Tables 1 and 2). The general synthetic scheme for this class of compounds is shown in Scheme 1, and detailed experimental procedures are provided in the Supporting Information for all intermediates and final compounds as well as compound **1**. Briefly, compound **1** underwent TFA-mediated *boc*-deprotection followed by HATU amide coupling to afford intermediate **2**. Subsequent benzyloxycarbonyl removal via hydrogen over palladium reduction gave key intermediate **3**, which was subjected to either reductive amination with assorted aryl aldehydes to afford compounds **5−12** or an

S_N2 reaction with 3,4-difluorobenzyl bromide to provide compound **4**. To obtain azetidine amides **17−33**, commercially available *tert*-butyl 2,7-diazaspiro[3.5]nonane-2-carboxylate was subjected to reductive amination with 6-fluoro-1*H*-indole-3-carbaldehyde to give intermediate **15**. *Boc*-deprotection with TFA afforded **16**, which then underwent HATU amide coupling with assorted aryl carboxylic acids to give compounds **17−34**.

Overall, this focused collection of spirocyclic antagonists provided a number of valuable SAR insights. With respect to the southern region, replacing the difluorophenyl moiety with the analogous dichlorophenyl substituent (**9**) resulted in significantly increased activity; however, a significant decrease in selectivity between the DR subtypes was also observed. Incorporation of other substituted arenes, such as fluorophenol (**8**), benzodioxole (**11**), and fluoropyridine (**10**), resulted in a steep decrease in inhibition (Table 1). By installing a 6-fluoroindole heterocycle (**5**) as we used previously in our morpholine core D₄R antagonist (VU6004432, Figure 1),[58] we observed drastically improved activity over **4**, though the overall selectivity was mildly decreased. Exchanging the indole for an indazole **6** resulted in an improvement in the selectivity against all subtypes, with a mild improvement in activity at D₄.₄R. This is in stark contrast to the incorporation of benzisoxazole (**7**), which essentially abolishes activity. Modifications to the spirocyclic core were not favorable as the addition of methyl groups to the 2 or 3 position of the piperidine ring (compounds **14** and **13**, respectively) significantly reduced the potency and affinity of the compound compared to that observed with **5** (Table 1), while expansion
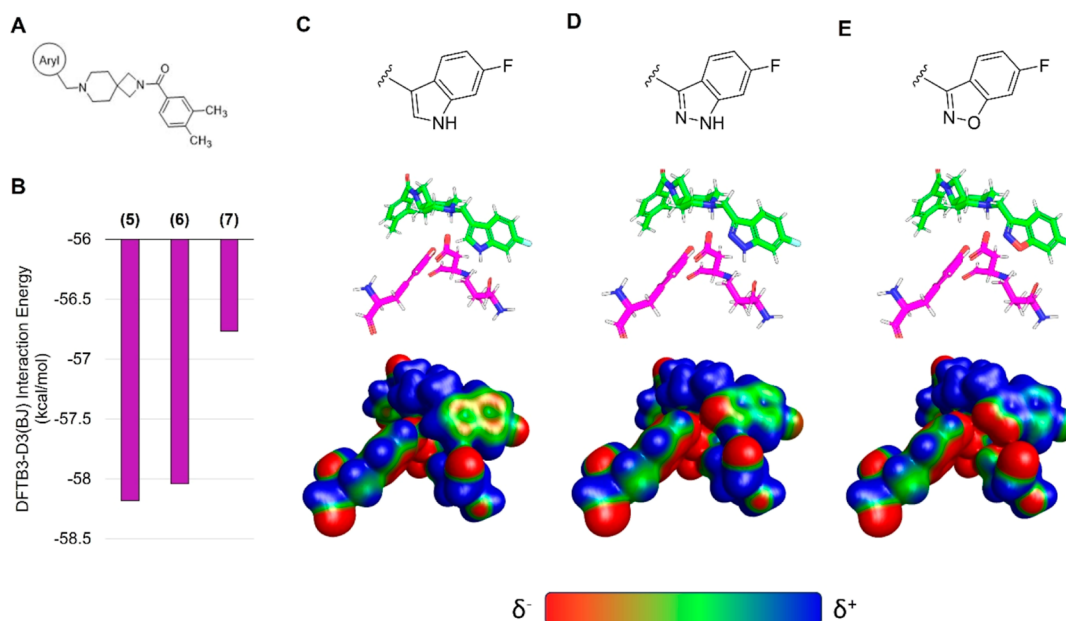
Figure 4. Surface electrostatics analysis of D_4R selective antagonists in complex with D_4R. (A) Schematic southern aryl substitution on compound **4**. (B) Interaction energies for the model systems containing compounds **5**, **6**, or **7**. Surface electrostatic potential analysis of (C) compound **5**, (D) compound **6**, and (E) compound **7**. Electrostatic potentials are calculated for model systems (C−D) at the wB97X-D/6-31G(d) level of theory with solvation model density (SMD) aqueous implicit solvent following geometry optimization of the receptor pocket and ligand in complex utilizing DFTB3-D3(BJ) with SMD solvent water.

of the azetidine to a pyrrolidine led to a substantial decrease in inhibitory activity (compound **42**; see Supporting Information).

To better understand the differences in activity between **5**, **6**, and **7**, we first docked **5** to D_4R. Once again, pseudosymmetry within **5** rendered two flipped binding modes plausible. The first binding mode (Figure 3E) follows from the predicted poses of *VU6052469* and **4**. Interestingly, however, an alternative binding mode in which the indole ring of **5** adopts a pose mimicking the experimentally determined bound pose of L745,870[68] is also possible. To determine which pose is more likely, we performed MD simulations starting from each docked pose. We observed that the pose consistent with **4** (Figure 3E) is more likely to remain near the docked binding pose (Figure S107A,B) and adopt favorable hydrogen bond geometry with D3.32 (Figure S107C,D). Furthermore, the interaction energy rankings for this binding mode (Figure 3E) are consistent with the experimental results and demonstrate the activity cliff in **7** (Table 1 and Figure 4A,B). In contrast, the binding mode mimicking the L745,870 pose yields interaction energy estimates inconsistent with experiment (data not shown). Visualization of the surface electrostatic potentials of D_4R complexed with **5**, **6**, or **7** at the DFT wB97X-D/6-31G(d) level of theory[72] suggests that this activity cliff is due to loss of complementary electrostatic interactions and an abundance of anionic charge near TM2 (Figure 4C−E).

While indazole antagonist **6** provided the best potency and selectivity profile thus far, we proceeded with the combination of the 6-fluoroindole southern ring and the unmodified 2,7-diazaspiro[3.5]nonane core for exploration of the northern region SAR as **5** performed similarly and was more cost-effective for library synthesis. Therefore, we employed **5** as a starting point for pursuing a focused library of aryl amides on the northern end of the scaffold for further improvement of DR subtype selectivity (Table 2). Overall, alkyl and chloro substituents were well-tolerated, with the sole exception of the 3,5-dichlorophenyl analogue (**28**), which demonstrated drastically reduced inhibitory activity (49%). The 2,4-dichlorophenyl regioisomer (**19**) retained activity, however, indicating that $D_{4.4}R$ inhibition is sensitive to subtle changes in substitution pattern in this region. In contrast to alkyl and chloro groups, incorporation of alkoxy groups generally led to a significant reduction in activity against $D_{4.4}R$ (**23−26**), with the sole exception being **20** (Figure 3F), which bears a benzodioxole heterocycle ($D_{4.4}R$ IC_{50} = 84 nM; K_i = 23 nM). The potency of benzodioxole-bearing compound **20** suggests that the lack of activity observed in compounds **23−26** is a result of unfavorable steric interactions facilitated by their freely rotating alkyl groups rather than ring electronics. In addition to the benzodioxole example (**20**), increasing the size of the aryl amide from a monocycle to a fused bicycle in other instances was also well tolerated (**27**, **31**), with naphthalene **27** exhibiting particularly potent activity ($D_{4.4}R$ IC_{50} = 28 nM; K_i = 7.6 nM). With respect to selectivity, a strong sensitivity to regioisomerism was observed, which was most clearly demonstrated in compounds **29**, **32**, and **33**, which bear *para*-, *meta*-, and *ortho*-toluamides, respectively. Of these, compound **29** demonstrates the highest $D_{4.4}R$ activity ($D_{4.4}R$ IC_{50} = 62 nM; K_i = 17 nM), and it exhibits a moderately improved selectivity profile over **5**. Both *meta* and *ortho* isomers (compounds **32** and **33**, respectively) display reduced activity compared to *para* isomer **29**. Compound **33** (Figure 3G), however, exhibited the best selectivity profile of all compounds disclosed herein, with a notable 0% activity against D_{2S}. It was also observed that replacement of the *para*-toluamide of **29** with a tosylamide (**34**) mildly reduced the $D_{4.4}R$ activity but notably increased the inhibitory activity at all other tested DR subtypes, possibly due to the reduced planarity of the sulfonamide.

Table 3. In Vivo and In Vitro Results of Selected Compounds

compound	$f_{u,plasma}{}^{a}$		$CL_H{}^{a}$ (mL/min/kg)		$CL_p{}^{a}$ (mL/min/kg)	$t_{1/2}{}^{a}$ (h)	$V_{ss}{}^{a}$ (L/kg)	AUC^{a} (h·ng/mL)
	human	rat	human	rat				
4	0.01	0.03	16.9	59.1	116	1.05	5.52	28.7
33	0.19	0.26	16.0	39.0	123	4.02	36.9	27.0
32	0.06	0.14	14.7	46.2				
29	0.05	0.15	17.3	49.2				
20	0.10	0.23	13.7	36.2	126	4.55	44.4	26.4

$^{a}f_u$ = Fraction unbound; equilibrium dialysis assay; CL_H = hepatic clearance; CL_p = plasma clearance; $t_{1/2}$ = terminal phase plasma half-life; V_{ss} = volume of distribution at steady-state; AUC = area under the curve.
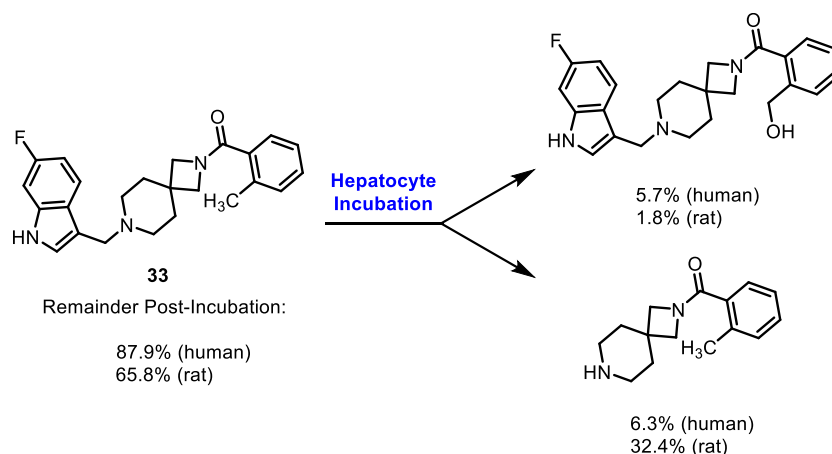
Figure 5. Metabolite analysis of compound **33** in human and rat hepatocytes. Parent compound incubated in human or rat hepatocytes for 4 h. Percentages (determined via LC/MS) indicate the relative percentage of compounds present postincubation. See Supporting Information for details.

In Vitro and In Vivo DMPK Analysis of Selected Compounds. A subset of compounds that demonstrated high potency and excellent selectivity were selected for pharmacokinetic characterization (Table 3). In vitro stability experiments in rat and human microsomes returned high clearance (>70% Q_h) across all compounds, except for **20**, which exhibited moderate hepatic clearance (CL_H of 13.7 and 36.2 in human and rat microsomes, respectively). The free fraction in plasma ranged from 1 to 19% in rat and 3−26% in human. Notably, both compounds **33** and **20** exhibited increased free fractions compared to the original hit (**4**). Three compounds (**4**, **20**, and **33**) were selected to assess in vivo pharmacokinetics (compounds **29** and **32** were excluded as they exhibited worse free fraction in plasma compared to **20** and **33**). Upon intravenous dosing in rats, all three compounds demonstrated superhepatic clearance (>100% Q_h). This result is consistent with these compounds experiencing high hepatic metabolic clearance and may also indicate contribution to clearance through a different route, such as extrahepatic metabolism or active direct excretion. Despite high clearance, compounds **4**, **20**, and **33** exhibited moderate to high distribution into tissues (volume of distributions of 5.52, 44.4, and 36.9 L/kg, respectively), explaining the reasonable half-lives for these compounds (1.05, 4.55, and 4.02 h, respectively).

Compound **33** was subjected to metabolite profiling in human and rat hepatocytes to provide insight into potential clearance mechanisms and metabolic liabilities (Figure 5). After incubation for 4 h, **33** exhibited low turnover in human hepatocytes and moderate turnover in rat hepatocytes, with 87.9 and 65.8% of parent compound (**33**) remaining postincubation, respectively. In both species, only two major metabolites were observed: mono-oxidation of the benzylic methyl group and piperidine N-dealkylation. The latter means of metabolism was elevated in rats (32.4%) compared to that in humans (6.3%).

DISCUSSION

The application of spirocycles to drug discovery efforts has increased in recent years as a means to increase compound three-dimensionality, modulate DMPK properties, incorporate additional sp^3 centers, and generate novel intellectual property.[75−78] One of the central findings of the present study was the discovery of 2,7-diazaspiro[3.5]nonane as an applicable core motif for selective D_4R antagonists. While we initially identified the highly potent antagonist *VU6052469*, which exhibited a high degree of structural similarity to a previously reported selective D_4R antagonist,[71] it notably lacked selectivity (Figure 2B,D,E). We postulated that this lack of selectivity arose from the difference in length between these two compounds, with the naphthalene and 4-chlorobenzyl moieties of the Carato compound potentially leading to poorer steric interactions within the TM2/3 pocket of D_2R than the dimethylphenyl and 3,4-difluorobenzyl moieties of *VU6052469* (Figure 2E). By replacing the core piperidine of *VU6052469* with 2,7-diazaspiro[3.5]nonane, the dimethylphenyl ring is extended further into the TM4/5/6 pocket, affording potent and selective activity against D_4R (Table 1). While there have been reported examples of substituted diazaspirocycles bearing D_4R activity, this activity was not the desired mode of action (i.e., the intent was to target σ receptors) nor did the more potent compounds exhibit DR subtype selectivity.[79] Therefore,

to the best of our knowledge, this is the first report of the use of diazaspirocycles in pursuit of selective D_4R antagonists.

Interestingly, our investigation revealed an activity cliff when comparing the indole/indazole- vs benzisoxazole-substituted compounds (compounds **5/6** and **7**, respectively). Activity cliffs are subtle structural changes leading to significant alterations in inhibitory activity. In this case, the subtle difference in ligand interaction energies with the receptor went undetected by the docking score function. It was only after performing geometry optimization and interaction energy calculations with the more computationally demanding semiempirical QM method DFTB3-D3(BJ) that we understood the case of the reduction in binding affinity, which was a result of an accumulation of anionic charge near TM2 with no available hydrogen bond donors. This example emphasizes the continued importance of developing force fields and/or deep learning algorithms for binding affinity prediction that can be used during rapid screening protocols.

A key challenge in the rational design of selective D_4R antagonists is the topological pseudosymmetry displayed by most antagonists. This challenge is 2-fold: (1) highly similar antagonists may be oriented in conformations 180° opposed to one another, and (2) the internal pseudosymmetry of many D_4R antagonists renders it difficult to ascertain their appropriate binding modes. Despite extensive computational validation, it is possible that our putative binding modes are inaccurate, which may lead to false structure−activity relationships. Further experimental structural evidence, such as crystal structures of these spirocyclic antagonists bound to D_4R, will be valuable in the design of future D_4R antagonists with similar potencies and selectivity.

Modifications to the northern aryl amide of this scaffold demonstrated the sensitivity of D_4R potency and selectivity to ring substituent choice and regioisomerism. Overall, compound **33**, which bears an *ortho*-toluamide northern substituent, displayed the best selectivity profile of the tested compounds while retaining potent $D_{4.4}R$ antagonism and affinity (IC_{50} = 210 nM; K_i = 59 nM). Though our study has yielded promising D_4R antagonists such as this, an ongoing challenge in the design of this class of compounds is the optimization of pharmacokinetic properties. While this class of compounds exhibited excellent aqueous solubility (see Supporting Information), both in vitro and in vivo pharmacokinetic analysis of selected compounds demonstrated a key limitation of the present class: high metabolic clearance. The findings of these assays underscore the need for continued efforts to improve the pharmacokinetic profiles of potential D_4R antagonist drug candidates, most likely via design changes to remove metabolic hotspots within this chemical series.

Altogether, our study has unveiled a spirocyclic core for D_4R selective antagonists, providing a foundation for further drug development efforts in the context of PD. Our insight into DR subtype selectivity and activity cliffs offers valuable guidance for future research in this area. The improvement of spirocyclic D_4R antagonist DMPK properties, however, remains requisite for the development of a suitable preclinical lead within this class as a potential adjuvant therapy for PD.

■ ASSOCIATED CONTENT

Ⓢ Supporting Information

The Supporting Information is available free of charge at https://pubs.acs.org/doi/10.1021/acschemneuro.4c00086.

Experimental procedure for the synthesis of compounds, ^1H and $^{13}C\{^1H\}$ NMR spectra for all compounds, 2D NMR (NOESY, HMBC, HSQC, and COSY) for compounds that required further characterization, DMPK experimental methods, computational methods, and metabolite profiling (PDF)

■ AUTHOR INFORMATION

Corresponding Authors

Craig W. Lindsley − *Warren Center for Neuroscience Drug Discovery and Department of Pharmacology, Vanderbilt University School of Medicine, Nashville, Tennessee 37232, United States; Department of Chemistry, Vanderbilt University, Nashville, Tennessee 37232, United States;* ⓞ orcid.org/0000-0003-0168-1445; Email: craig.lindsley@vanderbilt.edu

Jens Meiler − *Department of Chemistry, Center for Structural Biology, and Center for Applied AI in Protein Dynamics, Vanderbilt University, Nashville, Tennessee 37232, United States; Institute for Drug Discovery, Leipzig University Medical School, Leipzig SAC 04103, Germany;* Email: jens.meiler@vanderbilt.edu

Caleb A. H. Jones − *Warren Center for Neuroscience Drug Discovery and Department of Pharmacology, Vanderbilt University School of Medicine, Nashville, Tennessee 37232, United States; Department of Chemistry, Vanderbilt University, Nashville, Tennessee 37232, United States;* ⓞ orcid.org/0000-0002-0471-9392; Email: caleb.a.jones@vanderbilt.edu

Authors

Benjamin P. Brown − *Department of Chemistry, Center for Structural Biology, and Center for Applied AI in Protein Dynamics, Vanderbilt University, Nashville, Tennessee 37232, United States*

Daniel C. Schultz − *Warren Center for Neuroscience Drug Discovery and Department of Pharmacology, Vanderbilt University School of Medicine, Nashville, Tennessee 37232, United States; Department of Chemistry, Vanderbilt University, Nashville, Tennessee 37232, United States*

Julie Engers − *Warren Center for Neuroscience Drug Discovery and Department of Pharmacology, Vanderbilt University School of Medicine, Nashville, Tennessee 37232, United States; Department of Chemistry, Vanderbilt University, Nashville, Tennessee 37232, United States*

Valerie M. Kramlinger − *Warren Center for Neuroscience Drug Discovery and Department of Pharmacology, Vanderbilt University School of Medicine, Nashville, Tennessee 37232, United States; Department of Chemistry, Vanderbilt University, Nashville, Tennessee 37232, United States*

Complete contact information is available at:
https://pubs.acs.org/10.1021/acschemneuro.4c00086

Author Contributions

¶C.A.H.J., B.P.B., and D.C.S. contributed equally to this work and are listed as co-first authors. C.A.H.J. and D.C.S. contributed to the synthesis and characterization of all the compounds. B.P.B. contributed through the modeling of the various D_4R antagonists in silico. J.E. organized the samples shipment to Eurofins and worked up the data for percent inhibition, K_i and IC_{50}. V.M.K. contributed by the design and

■ **REFERENCES**

(1) Gelb, D. J.; Oliver, E.; Gilman, S. Diagnostic Criteria for Parkinson Disease. *Arch. Neurol.* **1999**, *56* (1), 33.

(2) Lee, T. K.; Yankee, E. L. A Review on Parkinson's Disease Treatment. *Neuroimmunol. Neuroinflammation* **2022**, *8*, 222.

(3) Huot, P.; Johnston, T. H.; Koprich, J. B.; Fox, S. H.; Brotchie, J. M. The Pharmacology of L-DOPA-Induced Dyskinesia in Parkinson's Disease. *Pharmacol. Rev.* **2013**, *65* (1), 171−222.

(4) Sebastianutto, I.; Maslava, N.; Hopkins, C. R.; Cenci, M. A. Validation of an Improved Scale for Rating L-DOPA-Induced Dyskinesia in the Mouse and Effects of Specific Dopamine Receptor Antagonists. *Neurobiol. Dis.* **2016**, *96*, 156−170.

(5) Lindsley, C. W.; Hopkins, C. R. Return of D_4 Dopamine Receptor Antagonists in Drug Discovery: Miniperspective. *J. Med. Chem.* **2017**, *60* (17), 7233−7243.

(6) Giorgioni, G.; Del Bello, F.; Pavletić, P.; Quaglia, W.; Botticelli, L.; Cifani, C.; Micioni Di Bonaventura, E.; Micioni Di Bonaventura, M. V.; Piergentili, A. Recent Findings Leading to the Discovery of Selective Dopamine D4 Receptor Ligands for the Treatment of Widespread Diseases. *Eur. J. Med. Chem.* **2021**, *212*, 113141.

(7) Kebabian, J. W. Multiple Classes of Dopamine Receptors in Mammalian Central Nervous System: The Involvement of Dopamine-Sensitive Adenylyl Cyclase. *Life Sci.* **1978**, *23* (5), 479−483.

(8) Missale, C.; Nash, S. R.; Robinson, S. W.; Jaber, M.; Caron, M. G. Dopamine Receptors: From Structure to Function. *Physiol. Rev.* **1998**, *78* (1), 189−225.

(9) Vallone, D.; Picetti, R.; Borrelli, E. Structure and Function of Dopamine Receptors. *Neurosci. Biobehav. Rev.* **2000**, *24* (1), 125−132.

(10) Tol, H. H. M. V.; Wu, C. M.; Guan, H.-C.; Ohara, K.; Bunzow, J. R.; Civelli, O.; Kennedy, J.; Seeman, P.; Niznik, H. B.; Jovanovic, V. Multiple Dopamine D4 Receptor Variants in the Human Population. *Nature* **1992**, *358* (6382), 149−152.

(11) Chang, F.-M.; Kidd, J. R.; Livak, K. J.; Pakstis, A. J.; Kidd, K. K. The World-Wide Distribution of Allele Frequencies at the Human Dopamine D4 Receptor Locus. *Hum. Genet.* **1996**, *98* (1), 91−101.

(12) Ding, Y.-C.; Chi, H.-C.; Grady, D. L.; Morishima, A.; Kidd, J. R.; Kidd, K. K.; Flodman, P.; Spence, M. A.; Schuck, S.; Swanson, J. M.; Zhang, Y.-P.; Moyzis, R. K. Evidence of Positive Selection Acting at the Human Dopamine Receptor D4 Gene Locus. *Proc. Natl. Acad. Sci. U.S.A.* **2002**, *99* (1), 309−314.

(13) Schneider, C. S.; Mierau, J. Dopamine Autoreceptor Agonists: Resolution and Pharmacological Activity of 2,6-Diaminotetrahydrobenzothiazole and an Aminothiazole Analog of Apomorphine. *J. Med. Chem.* **1987**, *30* (3), 494−498.

(14) Mierau, J.; Schingnitz, G. Biochemical and Pharmacological Studies on Pramipexole, a Potent and Selective Dopamine D2 Receptor Agonist. *Eur. J. Pharmacol.* **1992**, *215* (2−3), 161−170.

(15) Mierau, J.; Schneider, F. J.; Ensinger, H. A.; Chio, C. L.; Lajiness, M. E.; Huff, R. M. Pramipexole Binding and Activation of Cloned and Expressed Dopamine D2, D3 and D4 Receptors. *Eur. J. Pharmacol., Mol. Pharmacol. Sect.* **1995**, *290* (1), 29−36.

(16) Bennett, J. P.; Piercey, M. F. Pramipexole — a New Dopamine Agonist for the Treatment of Parkinson's Disease. *J. Neurol. Sci.* **1999**, *163* (1), 25−31.

(17) Antonini, A.; Barone, P.; Ceravolo, R.; Fabbrini, G.; Tinazzi, M.; Abbruzzese, G. Role of Pramipexole in the Management of Parkinson's Disease: *CNS Drugs* **2010**, *24* (10), 829−841.

(18) Frampton, J. E. Pramipexole Extended-Release: A Review of Its Use in Patients with Parkinson's Disease. *Drugs* **2014**, *74* (18), 2175−2190.

(19) Gallagher, G.; Lavanchy, P. G.; Wilson, J. W.; Hieble, J. P.; DeMarinis, R. M. 4-[2-(Di-n-Propylamino)Ethyl]-2(3H)-Indolone: A Prejunctional Dopamine Receptor Agonist. *J. Med. Chem.* **1985**, *28* (10), 1533−1536.

(20) Eden, R. J.; Costall, B.; Domeney, A. M.; Gerrard, P. A.; Harvey, C. A.; Kelly, M. E.; Naylor, R. J.; Owen, D. A. A.; Wright, A. Preclinical Pharmacology of Ropinirole (SK&F 101468-A) a Novel Dopamine D2 Agonist. *Pharmacol., Biochem. Behav.* **1991**, *38* (1), 147−154.

(21) Stacy, M. Update on ropinirole in the treatment of Parkinson&rsquo;s disease. *Neuropsychiatr. Dis. Treat.* **2008**, *33*, 33.

(22) Funk, C. LXV.—Synthesis of Dl-3:4-Dihydroxyphenylalanine. *J. Chem. Soc., Trans.* **1911**, *99* (0), 554−557.

(23) Birkmayer, W.; Hornykiewicz, O. The L-3,4-dioxyphenylalanine (DOPA)-effect in Parkinson-akinesia. *Wien. Klin. Wochenschr.* **1961**, *73*, 787−788.

(24) Hornykiewicz, O. L-DOPA: From a Biologically Inactive Amino Acid to a Successful Therapeutic Agent. *Amino Acids* **2002**, *23* (1−3), 65−70.

(25) Tambasco, N.; Romoli, M.; Calabresi, P. Levodopa in Parkinson's Disease: Current Status and Future Developments. *Curr. Neuropharmacol.* **2018**, *16* (8), 1239−1252.

(26) Thomas, T. C.; Kruzich, P. J.; Joyce, B. M.; Gash, C. R.; Suchland, K.; Surgener, S. P.; Rutherford, E. C.; Grandy, D. K.; Gerhardt, G. A.; Glaser, P. E. A. Dopamine D4 Receptor Knockout Mice Exhibit Neurochemical Changes Consistent with Decreased Dopamine Release. *J. Neurosci. Methods* **2007**, *166* (2), 306−314.

(27) Friedman, N. P.; Robbins, T. W. The Role of Prefrontal Cortex in Cognitive Control and Executive Function. *Neuropsychopharmacology* **2022**, *47* (1), 72−89.

(28) Rajmohan, V.; Mohandas, E. The Limbic System. *Indian J. Psychiatry* **2007**, *49* (2), 132−139.

(29) O'Malley, K. L.; Harmon, S.; Tang, L.; Todd, R. D. The Rat Dopamine D4 Receptor: Sequence, Gene Structure, and Demonstration of Expression in the Cardiovascular System. *New Biol.* **1992**, *4* (2), 137−146.

(30) Van Tol, H. H. M.; Bunzow, J. R.; Guan, H.-C.; Sunahara, R. K.; Seeman, P.; Niznik, H. B.; Civelli, O. Cloning of the Gene for a Human Dopamine D4 Receptor with High Affinity for the Antipsychotic Clozapine. *Nature* **1991**, *350* (6319), 610−614.

(31) Cohen, A. I.; Todd, R. D.; Harmon, S.; O'Malley, K. L. Photoreceptors of Mouse Retinas Possess D4 Receptors Coupled to

Adenylate Cyclase. *Proc. Natl. Acad. Sci. U.S.A.* **1992**, *89* (24), 12093–12097.

(32) Matsumoto, M.; Hidaka, K.; Tada, S.; Tasaki, Y.; Yamaguchi, T. Full-Length cDNA Cloning and Distribution of Human Dopamine D4 Receptor. *Mol. Brain Res.* **1995**, *29* (1), 157–162.

(33) Mrzljak, L.; Bergson, C.; Pappy, M.; Huff, R.; Levenson, R.; Goldman-Rakic, P. S. Localization of Dopamine D4 Receptors in GABAergic Neurons of the Primate Brain. *Nature* **1996**, *381* (6579), 245–248.

(34) Ariano, M. A.; Wang, J.; Noblett, K. L.; Larson, E. R.; Sibley, D. R. Cellular Distribution of the Rat D4 Dopamine Receptor Protein in the CNS Using Anti-Receptor Antisera. *Brain Res.* **1997**, *752* (1–2), 26–34.

(35) Ptacek, R.; Kuzelova, H.; Stefano, G. B. Dopamine D4 Receptor Gene DRD4 and Its Association with Psychiatric Disorders. *Med. Sci. Monit.* **2011**, *17* (9), RA215–RA220.

(36) Defagot, M. C.; Falzone, T. L.; Low, M. J.; Grandy, D. K.; Rubinstein, M.; Antonelli, M. C. Quantitative Analysis of the Dopamine D4 Receptor in the Mouse Brain. *J. Neurosci. Res.* **2000**, *59* (2), 202–208.

(37) Meador-Woodruff, J. H. Dopamine Receptor Transcript Expression in Striatum and Prefrontal and Occipital Cortex: Focal Abnormalities in Orbitofrontal Cortex in Schizophrenia. *Arch. Gen. Psychiatry* **1997**, *54* (12), 1089.

(38) Lidow, M. S.; Wang, F.; Cao, Y.; Goldman-Rakic, P. S. Layer V Neurons Bear the Majority of mRNAs Encoding the Five Distinct Dopamine Receptor Subtypes in the Primate Prefrontal Cortex. *Synapse* **1998**, *28* (1), 10–20.

(39) Primus, R. J.; Thurkauf, A.; Xu, J.; Yevich, E.; McInerney, S.; Shaw, K.; Tallman, J. F.; Gallagher, D. W. II. Localization and Characterization of Dopamine D4 Binding Sites in Rat and Human Brain by Use of the Novel, D4 Receptor-Selective Ligand [3H]NGD 94–1. *J. Pharmacol. Exp. Ther.* **1997**, *282* (2), 1020–1027.

(40) Meador-Woodruff, J. H.; Grandy, D. K.; Van Tol, H. H. M.; Damask, S. P.; Little, K. Y.; Civelli, O.; Watson, S. J. Dopamine Receptor Gene Expression in the Human Medial Temporal Lobe. *Neuropsychopharmacology* **1994**, *10* (4), 239–248.

(41) Di Ciano, P.; Grandy, D. K.; Le Foll, B. Dopamine D4 Receptors in Psychostimulant Addiction. *Advances in Pharmacology*; Elsevier, 2014; Vol. 69, pp 301–321..

(42) Gornick, M. C.; Addington, A.; Shaw, P.; Bobb, A. J.; Sharp, W.; Greenstein, D.; Arepalli, S.; Castellanos, F. X.; Rapoport, J. L. Association of the Dopamine Receptor D4 (*DRD4*) Gene 7-repeat Allele with Children with Attention-deficit/Hyperactivity Disorder (ADHD): An Update. *Am. J. Med. Genet., Part B* **2007**, *144B* (3), 379–382.

(43) Zhang, K.; Davids, E.; Tarazi, F.; Baldessarini, R. Effects of Dopamine D4 Receptor-Selective Antagonists on Motor Hyperactivity in Rats with Neonatal 6-Hydroxydopamine Lesions. *Psychopharmacology* **2002**, *161* (1), 100–106.

(44) Avale, M. E.; Falzone, T. L.; Gelman, D. M.; Low, M. J.; Grandy, D. K.; Rubinstein, M. The Dopamine D4 Receptor Is Essential for Hyperactivity and Impaired Behavioral Inhibition in a Mouse Model of Attention Deficit/Hyperactivity Disorder. *Mol. Psychiatry* **2004**, *9* (7), 718–726.

(45) Huot, P.; Johnston, T. H.; Koprich, J. B.; Aman, A.; Fox, S. H.; Brotchie, J. M. L-745,870 Reduces L-DOPA-Induced Dyskinesia in the 1-Methyl-4-Phenyl-1,2,3,6-Tetrahydropyridine-Lesioned Macaque Model of Parkinson's Disease. *J. Pharmacol. Exp. Ther.* **2012**, *342* (2), 576–585.

(46) Erlij, D.; Acosta-García, J.; Rojas-Márquez, M.; González-Hernández, B.; Escartín-Perez, E.; Aceves, J.; Florán, B. Dopamine D4 Receptor Stimulation in GABAergic Projections of the Globus Pallidus to the Reticular Thalamic Nucleus and the Substantia Nigra Reticulata of the Rat Decreases Locomotor Activity. *Neuropharmacology* **2012**, *62* (2), 1111–1118.

(47) Bastide, M. F.; Meissner, W. G.; Picconi, B.; Fasano, S.; Fernagut, P.-O.; Feyder, M.; Francardo, V.; Alcacer, C.; Ding, Y.; Brambilla, R.; Fisone, G.; Jon Stoessl, A.; Bourdenx, M.; Engeln, M.; Navailles, S.; De Deurwaerdère, P.; Ko, W. K. D.; Simola, N.; Morelli, M.; Groc, L.; Rodriguez, M.-C.; Gurevich, E. V.; Quik, M.; Morari, M.; Mellone, M.; Gardoni, F.; Tronci, E.; Guehl, D.; Tison, F.; Crossman, A. R.; Kang, U. J.; Steece-Collier, K.; Fox, S.; Carta, M.; Angela Cenci, M.; Bézard, E. Pathophysiology of L-Dopa-Induced Motor and Non-Motor Complications in Parkinson's Disease. *Prog. Neurobiol.* **2015**, *132*, 96–168.

(48) Conde Rojas, I.; Acosta-García, J.; Caballero-Florán, R. N.; Jijón-Lorenzo, R.; Recillas-Morales, S.; Avalos-Fuentes, J. A.; Paz-Bermúdez, F.; Leyva-Gómez, G.; Cortés, H.; Florán, B. Dopamine D4 Receptor Modulates Inhibitory Transmission in Pallido-pallidal Terminals and Regulates Motor Behavior. *Eur. J. Neurosci.* **2020**, *52* (11), 4563–4585.

(49) Coward, D. M. General Pharmacology of Clozapine. *Br. J. Psychiatry* **1992**, *160* (S17), 5–11.

(50) Patel, S.; Freedman, S.; Chapman, K. L.; Emms, F.; Fletcher, A. E.; Knowles, M.; Marwood, R.; Mcallister, G.; Myers, J.; Curtis, N.; Kulagowski, J. J.; Leeson, P. D.; Ridgill, M.; Graham, M.; Matheson, S.; Rathbone, D.; Watt, A. P.; Bristow, L. J.; Rupniak, N. M.; Baskin, E.; Lynch, J. J.; Ragan, C. I. Biological Profile of L-745,870, a Selective Antagonist with High Affinity for the Dopamine D4 Receptor. *J. Pharmacol. Exp. Ther.* **1997**, *283* (2), 636–647.

(51) Kramer, M. S. The Effects of a Selective D4 Dopamine Receptor Antagonist (L-745,870) in Acutely Psychotic Inpatients With Schizophrenia. *Arch. Gen. Psychiatry* **1997**, *54* (6), 567.

(52) Bristow, L. J.; Collinson, N.; Cook, G. P.; Curtis, N.; Freedman, S. B.; Kulagowski, J. J.; Leeson, P. D.; Patel, S.; Ragan, C. I.; Ridgill, M.; Saywell, K. L.; Tricklebank, M. D. L-745,870, a Subtype Selective Dopamine D4 Receptor Antagonist, Does Not Exhibit a Neuroleptic-like Profile in Rodent Behavioral Tests. *J. Pharmacol. Exp. Ther.* **1997**, *283* (3), 1256–1263.

(53) Janssen, P. A. J.; Jageneau, A. H. M.; Schellekens, K. H. L. Chemistry and Pharmacology of Compounds Related to 4-(4-Hydroxy-4-Phenyl-Piperidino)-Butyrophenone: Part IV Influence of Haloperidol (R 1625) and of Chlorpromazine on the Behaviour of Rats in an Unfamiliar "Open Field" Situation. *Psychopharmacologia* **1960**, *1* (5), 389–392.

(54) Divry, P.; Bobon, J.; Collard, J.; Pinchard, A.; Nols, E. Study & clinical trial of R 1625 or haloperidol, a new neuroleptic & so-called neurodysleptic agent. *Acta Neurol. Psychiatr. Belg.* **1959**, *59* (3), 337–366.

(55) Janssen, P. A. J.; Van De Westeringh, C..; Jageneau, A. H. M.; Demoen, P. J. A.; Hermans, B. K. F.; Van Daele, G. H. P.; Schellekens, K. H. L.; Van Der Eycken, C. A. M.; Niemegeers, C. J. E. Chemistry and Pharmacology of CNS Depressants Related to 4-(4-Hydroxy-4-Phenylpiperidino)Butyrophenone Part I-Synthesis and Screening Data in Mice. *J. Med. Pharm. Chem.* **1959**, *1* (3), 281–297.

(56) Divry, P.; Bobon, J.; Collard, J. [R-1625: a new drug for the symptomatic treatment of psychomotor excitation]. *Acta Neurol. Psychiatr. Belg.* **1958**, *58* (10), 878–888.

(57) Sanner, M. A.; Chappie, T. A.; Dunaiskis, A. R.; Fliri, A. F.; Desai, K. A.; Zorn, S. H.; Jackson, E. R.; Johnson, C. G.; Morrone, J. M.; Seymour, P. A.; Majchrzak, M. J.; Stephen Faraci, W.; Collins, J. L.; Duignan, D. B.; Di Prete, C. C.; Lee, J. S.; Trozzi, A. Synthesis, Sar and Pharmacology of CP-293,019: A Potent, Selective Dopamine D4 Receptor Antagonist. *Bioorg. Med. Chem. Lett.* **1998**, *8* (7), 725–730.

(58) Witt, J. O.; McCollum, A. L.; Hurtado, M. A.; Huseman, E. D.; Jeffries, D. E.; Temple, K. J.; Plumley, H. C.; Blobaum, A. L.; Lindsley, C. W.; Hopkins, C. R. Synthesis and Characterization of a Series of Chiral Alkoxymethyl Morpholine Analogs as Dopamine Receptor 4 (D4R) Antagonists. *Bioorg. Med. Chem. Lett.* **2016**, *26* (10), 2481–2488.

(59) Tolentino, K. T.; Mashinson, V.; Vadukoot, A. K.; Hopkins, C. R. Discovery and Characterization of Benzyloxy Piperidine Based Dopamine 4 Receptor Antagonists. *Bioorg. Med. Chem. Lett.* **2022**, *61*, 128615.

(60) Ford, B.; Lynch, T.; Greene, P. Risperidone in Parkinson's Disease. *Lancet* **1994**, *344* (8923), 681.

(61) Friedman, J. H.; Berman, R. M.; Goetz, C. G.; Factor, S. A.; Ondo, W. G.; Wojcieszek, J.; Carson, W. H.; Marcus, R. N. Open-label Flexible-dose Pilot Study to Evaluate the Safety and Tolerability of Aripiprazole in Patients with Psychosis Associated with Parkinson's Disease. *Mov. Disord.* **2006**, *21* (12), 2078−2081.

(62) Kurtz, A. L.; Kaufer, D. I. Dementia in Parkinson's Disease. *Curr. Treat. Options Neurol.* **2011**, *13* (3), 242−254.

(63) Aubert, I.; Guigoni, C.; Håkansson, K.; Li, Q.; Dovero, S.; Barthe, N.; Bioulac, B. H.; Gross, C. E.; Fisone, G.; Bloch, B.; Bezard, E. Increased D_1 Dopamine Receptor Signaling in Levodopa-induced Dyskinesia. *Ann. Neurol.* **2005**, *57* (1), 17−26.

(64) Darmopil, S.; Martín, A. B.; De Diego, I. R.; Ares, S.; Moratalla, R. Genetic Inactivation of Dopamine D1 but Not D2 Receptors Inhibits L-DOPA-Induced Dyskinesia and Histone Activation. *Biol. Psychiatr.* **2009**, *66* (6), 603−613.

(65) Jeffries, D. E.; Witt, J. O.; McCollum, A. L.; Temple, K. J.; Hurtado, M. A.; Harp, J. M.; Blobaum, A. L.; Lindsley, C. W.; Hopkins, C. R. Discovery, Characterization and Biological Evaluation of a Novel (R)-4,4-Difluoropiperidine Scaffold as Dopamine Receptor 4 (D 4 R) Antagonists. *Bioorg. Med. Chem. Lett.* **2016**, *26* (23), 5757−5764.

(66) Berry, C. B.; Bubser, M.; Jones, C. K.; Hayes, J. P.; Wepy, J. A.; Locuson, C. W.; Daniels, J. S.; Lindsley, C. W.; Hopkins, C. R. Discovery and Characterization of ML398, a Potent and Selective Antagonist of the D_4 Receptor with *in Vivo* Activity. *ACS Med. Chem. Lett.* **2014**, *5* (9), 1060−1064.

(67) Boateng, C. A.; Nilson, A. N.; Placide, R.; Pham, M. L.; Jakobs, F. M.; Boldizsar, N.; McIntosh, S.; Stallings, L. S.; Korankyi, I. V.; Kelshikar, S.; Shah, N.; Panasis, D.; Muccilli, A.; Ladik, M.; Maslonka, B.; McBride, C.; Sanchez, M. X.; Akca, E.; Alkhatib, M.; Saez, J.; Nguyen, C.; Kurtyan, E.; DePierro, J.; Crowthers, R.; Brunt, D.; Bonifazi, A.; Newman, A. H.; Rais, R.; Slusher, B. S.; Free, R. B.; Sibley, D. R.; Stewart, K. D.; Wu, C.; Hemby, S. E.; Keck, T. M. Pharmacology and Therapeutic Potential of Benzothiazole Analogues for Cocaine Use Disorder. *J. Med. Chem.* **2023**, *66* (17), 12141−12162.

(68) Zhou, Y.; Cao, C.; He, L.; Wang, X.; Zhang, X. C. Crystal Structure of Dopamine Receptor D4 Bound to the Subtype Selective Ligand, L745870. *eLife* **2019**, *8*, No. e48822.

(69) Wang, S.; Wacker, D.; Levit, A.; Che, T.; Betz, R. M.; McCorvy, J. D.; Venkatakrishnan, A. J.; Huang, X.-P.; Dror, R. O.; Shoichet, B. K.; Roth, B. L. D_4 Dopamine Receptor High-Resolution Structures Enable the Discovery of Selective Agonists. *Science* **2017**, *358* (6361), 381−386.

(70) Brown, B. P.; Mendenhall, J.; Meiler, J. BCL::MolAlign: Three-Dimensional Small Molecule Alignment for Pharmacophore Mapping. *J. Chem. Inf. Model.* **2019**, *59* (2), 689−701.

(71) Carato, P.; Graulich, A.; Jensen, N.; Roth, B. L.; Liégeois, J. F. Synthesis and in Vitro Binding Studies of Substituted Piperidine Naphthamides. Part II: Influence of the Substitution on the Benzyl Moiety on the Affinity for D2L, D4.2, and 5-HT2A Receptors. *Bioorg. Med. Chem. Lett.* **2007**, *17* (6), 1570−1574.

(72) Chai, J.-D.; Head-Gordon, M. Long-Range Corrected Hybrid Density Functionals with Damped Atom-Atom Dispersion Corrections. *Phys. Chem. Chem. Phys.* **2008**, *10* (44), 6615.

(73) Gaus, M.; Cui, Q.; Elstner, M. DFTB3: Extension of the Self-Consistent-Charge Density-Functional Tight-Binding Method (SCC-DFTB). *J. Chem. Theory Comput.* **2011**, *7* (4), 931−948.

(74) Brandenburg, J. G.; Grimme, S. Accurate Modeling of Organic Molecular Crystals by Dispersion-Corrected Density Functional Tight Binding (DFTB). *J. Phys. Chem. Lett.* **2014**, *5* (11), 1785−1789.

(75) Lovering, F.; Bikker, J.; Humblet, C. Escape from Flatland: Increasing Saturation as an Approach to Improving Clinical Success. *J. Med. Chem.* **2009**, *52* (21), 6752−6756.

(76) Lovering, F. Escape from Flatland 2: Complexity and Promiscuity. *MedChemComm* **2013**, *4* (3), 515.

(77) Talele, T. T. Opportunities for Tapping into Three-Dimensional Chemical Space through a Quaternary Carbon. *J. Med. Chem.* **2020**, *63* (22), 13291−13315.

(78) Hiesinger, K.; Dar'in, D.; Proschak, E.; Krasavin, M. Spirocyclic Scaffolds in Medicinal Chemistry. *J. Med. Chem.* **2021**, *64* (1), 150−183.

(79) Tolentino, K. T.; Mashinson, V.; Sharma, M. K.; Chhonker, Y. S.; Murry, D. J.; Hopkins, C. R. From Dopamine 4 to Sigma 1: Synthesis, SAR and Biological Characterization of a Piperidine Scaffold of Σ1 Modulators. *Eur. J. Med. Chem.* **2022**, *244*, 114840.